Exploring the Limits of the Electrostatically Induced Conformational Folding Process in Charge-Separated Excited States: Retarding Effect of Long Alkyl Tails Attached to the Chromophores

Xavier Y. Lauteslager[a], Marcel J. Bartels[a], Jacob J. Piet[b], John M. Warman[b], Jan W. Verhoeven[a], and Albert M. Brouwer*[a]

Institute of Molecular Chemistry, University of Amsterdam[a],
Nieuwe Achtergracht 129, NL-1018 WS Amsterdam, The Netherlands

IRI, Delft University of Technology[b],
Mekelweg 15, NL-2629 JB Delft, The Netherlands

Received May 1, 1998

Keywords: Conformational dynamics / Electron transfer / Donor-acceptor systems / Harpooning / Charge-transfer fluorescence

Six new donor-bridge-acceptor compounds have been synthesized which contain a long *n*-tetradecyl chain attached to the donor or acceptor moiety, or to both of them. Systems **1**, **2**, and **3** are analogs of the fluorescent probe molecule Fluoroprobe (**4**). They contain a rigidly extended 4-methylenepiperidine bridge and show relatively strong charge transfer fluorescence in solvents of low and medium polarity. Systems **1a**, **2a**, and **3a** contain a semiflexible 4-methylpiperidine bridge, obtained after hydrogenation of the exocyclic double bond of **1**, **2** and **3**, respectively. These systems undergo a conformational change following photoinduced charge separation ("harpooning") in nonpolar solvents and probably also in solvents of medium polarity. Both the steady state fluorescence spectra and the fluorescence decay times of the extended charge transfer (ECT) species show that the photoinduced folding process is effectively slowed down by the introduction of the long alkyl tails. This is most pronounced for **1a** which has an *n*-tetradecyl group attached to both donor and acceptor. In solution a small difference in the rate of folding is observed between **2a** and **3a**, which have a single *n*-tetradecyl chain attached to the acceptor only and to the donor only, respectively.

Linked donor (D)−acceptor (A) systems of the type D−bridge−A, in which the bridge is a hydrocarbon moiety, have been developed into a major tool for studying various aspects of electron donor-acceptor interaction over the past decades. A long standing subject of debate has been the mechanism of formation of so-called internal exciplexes in such systems in which donor and acceptor adopt a "sandwich" conformation. In several piperidine-bridged donor-acceptor systems studied in our group by Wegewijs[1] and Scherer[2] substantial proof was obtained that an exciplex-like compact charge transfer (CCT) species with the bridging piperidine ring in a (twist)boat conformation is formed from an extended charge transfer (ECT) species in which donor and acceptor are well separated in space and that the formation of the ECT species involves a charge transfer process in which the molecule is still in the extended conformation with the piperidine ring in the preferred chair conformation. Crucial for the observation of this "harpooning" process for the formation of the CCT species was the fact that both the ECT and the CCT state show fluorescence.

The interconversion of the ECT into the CCT species for the systems studied by Wegewijs and Scherer is very fast at room temperature in nonpolar alkane solvents. However, by cooling the sample the folding process can be slowed down, as is expected for a thermally activated process like the chair-boat interconversion, which made it possible to follow the interconversion of the two species in a time-resolved fashion. The folding process requires a dramatic conformational change, and one therefore expects that the viscosity of the medium plays an important role. A pronounced viscosity effect, however, could only be observed for the system with the exocyclic CH_2 group (**4a**)[1a][3] and for systems with flexible trimethylene bridges[3a]. The more rigid systems, lacking the CH_2 group, do not show a viscosity effect on the folding process[2a].

Scheme 1. Schematic representation of the "harpooning" process

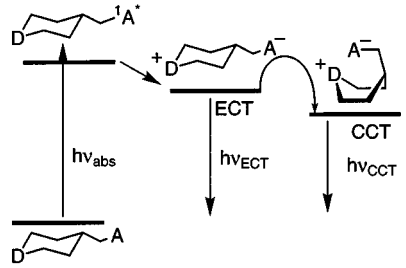

To further investigate the viscosity effect we devised some new systems with the same piperidine bridge and similar aniline donor and naphthalene acceptor chromophores. Because the folding process requires a large-scale molecular motion it is expected that the effect of viscosity will be more pronounced when the moving parts are more bulky. We therefore synthesized systems with long alkyl tails (C_{14}) attached to either donor or acceptor or to both of them. Al-

  1434−193X/98/1111−2467 $ 17.50+.50/0

Scheme 2. Molecular mechanics models of ECT and CCT species of **1a**; AM1/UHF/ESP charges were used, in combination with the Tripos force field

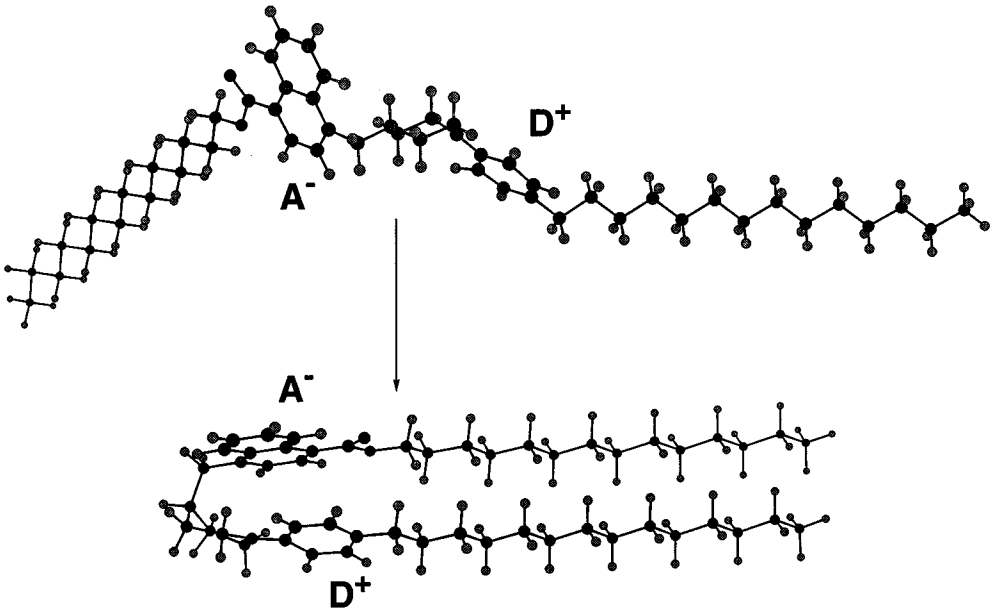

though in the folding process the naphthalene−aniline center-to-center distance is reduced by only ca. 2 Å, a leverage effect causes a large displacement of the alkyl tails, as illustrated in Scheme 2.

The synthetic strategy is covered in the next Section. The precursors of the new systems turned out to be highly fluorescent, making them in principle suitable to serve as probe molecules. The photophysical properties of these systems will be discussed below.

Synthesis

For the synthesis we used the same synthetic methodology which has been successfully applied many times in our group[4]. Coupling of an arylpiperidone with the methylphosphonate connected to the aromatic acceptor chromophore and subsequent reduction of the exocyclic double bond yields the desired systems. Two different piperidones, 1-*p*-tolylpiperidin-4-one and 1-(4-*n*-tetradecylphenyl)piperidin-4-one, were synthesized by cyclization of the appropriate anilines with 1,5-dichloro-3-pentanone. As a synthon for the acceptor chromophore lacking a tetradecyl chain, diethyl [(4-cyano-1-naphthyl)methyl]phosphonate was available[4]. In order to attach an *n*-tetradecyl chain to the acceptor moiety we used the carboxylic ester instead of the nitrile. Starting with 1-bromo-4-methylnaphthalene the Grignard reagent was prepared and converted into 4-methylnaphthalene-1-carboxylic acid. The acid was transformed to the acid chloride and condensed with *n*-tetradecanol. Bromination with *N*-bromosuccinimide and reaction with triethyl phosphite finally led to the desired phosphonate, *n*-tetradecyl 4-(diethoxy-phosphorylmethyl)naphthalene-1-carboxylate. The two piperidones and two phosphonates were coupled in three ways, leading to donor-acceptor systems with two tetradecyl chains attached to both chromophores, **1**, with only one tetradecyl chain attached to the acceptor, **2**, or with one tetradecyl chain attached to the donor, **3**. Hydrogenation of the double bond subsequently yields the semiflexible systems. The studied compounds are depicted in Scheme 3.

Electronic Absorption Spectra of the Donor-Acceptor Systems

The absorption spectra of all compounds were measured in cyclohexane. The spectra of **1** and **2** were virtually identical, which can be expected because the only difference is the size of the alkyl substituent, which does not alter the electronic properties of the aniline chromophore. The same holds for **1a** and **2a**. The spectra of **1** and **3** are given in Figure 1A. It is clear that replacement of the cyano group by an ester moiety does not alter the absorption spectrum significantly: only a small red-shift is observed of the longest wavelength π-π* transition of the acceptor from 309 nm in **3** to 311 nm in **1**.

The spectra of both compounds tail into the red, which might be caused by the presence of an underlying charge transfer absorption band of low intensity[5]. The spectra of **1a** and **3a** are given in Figure 1B. The main difference between these compounds and **1** and **3** is the hypsochromic shift of the long-wavelength absorption band of the acceptor due to the reduction of the size of its π-system. A striking difference between **1a** (and **2a**) compared to **3a** is the absence of fine-structure in the naphthalene absorption centered around 300 nm, so clearly observable in **3a**. This is probably due to inhomogeneous broadening resulting from the flexibility of the ester group. The 0−0 transition energy is virtually identical for both compounds.

Scheme 3. Compounds studied

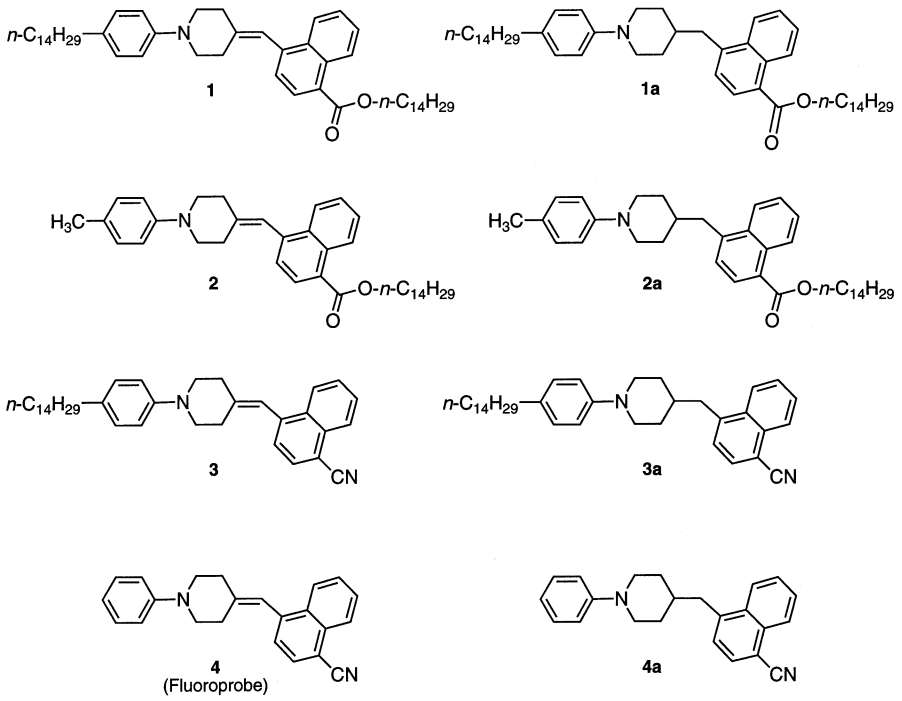

Figure 1. UV absorption spectra of **1** (full line) and **3** (dotted line) (A) and **1a** (full line) and **3a** (dotted line) (B) in cyclohexane

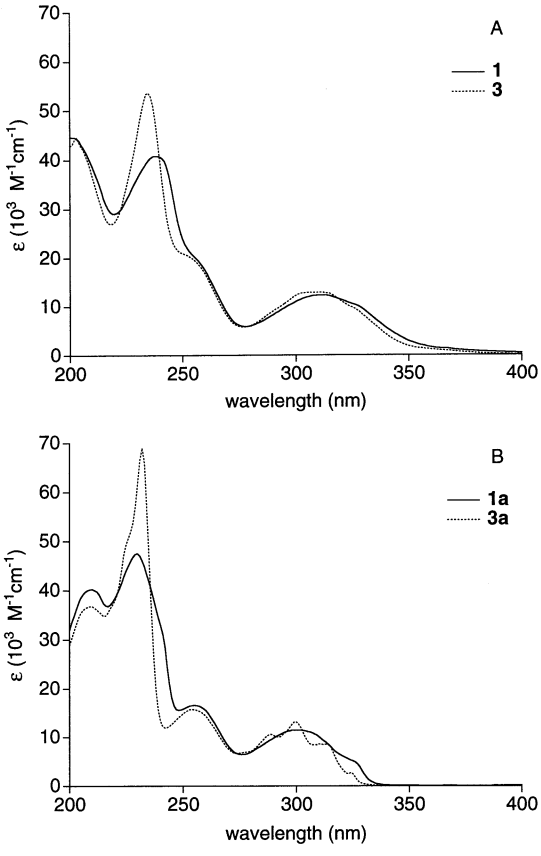

The electronic transitions observed in the absorption spectra are not seen in the fluorescence spectra of the donor-acceptor compounds, which invariably emit from a relaxed charge-transfer excited state. The fluorescence spectra characteristic of the naphthalene chromophores have been studied using 1-cyano-4-methylnaphthalene[2a] and the corresponding *n*-tetradecyl carboxylic ester. The fluorescence spectra have maxima at 338 and 346 nm in cyclohexane, and the quantum yields are 0.33[2a] and 0.08 for the nitrile and the ester, respectively.

Fluorescence of 1, 2, and 3

The fluorescence of compounds **1**, **2**, and **3** was measured in a range of solvents. Although excitation is in the lowest energy absorption band of the naphthalene chromophore, the corresponding fluorescence is not observed. A broad solvatochromic fluorescence is seen instead, which is ascribed to charge transfer fluorescence, as has been observed for similar systems[6]. The charge transfer fluorescence maxima, quantum yields and lifetimes are given in Table 1.

The solvent dependence of charge transfer fluorescence can be analyzed on the basis of dielectric continuum theory, using the Lippert-Mataga equation (1)[7]. In this equation the solvent dependence of the maximum of the charge transfer emission band ν_{CT} (in cm^{-1}) is correlated with the solvent polarity parameter Δf [equation (2)]. In equation (1) $\nu_{CT}(0)$ corresponds to the emission maximum in the gas phase, μ_{CT} (in Debye) is the dipole moment of the charge transfer state, *h* is Planck's constant, *c* is the velocity of light, ρ (in Å) is the effective radius of the solvent cavity

Table 1. Fluorescence maxima [nm], quantum yields and lifetimes [ns] for compounds **1**−**3** (excitation wavelength 308 nm) in various solvents

Solvent	Δf	**1** λ_{max}	**1** Φ_f	**1** τ_f	**2** λ_{max}	**2** Φ_f	**2** τ_f	**3** λ_{max}[a]	**3** Φ_f[a]	**3** τ_f
n-hexane	0.092	417	0.25	1.9	416	0.20	1.5[b]	417	0.55	4.8
cyclohexane	0.100	419	0.31	2.5	417	0.25	1.8[b]	421	0.59	5.5
benzene	0.116	490	0.69	13.6	494	0.62	13.5	496	0.63	14.2
di-*n*-pentyl ether	0.171	472	0.62	12	473	0.74	12.4	–	–	15.4
di-*n*-butyl ether	0.194	477	0.59	12	–	–	–	474	0.51	14.8
di-*n*-propyl ether	0.213	487	0.52	12	–	–	–	–	–	–
diisopropyl ether	0.237	495	0.44	12	499	0.39	13.1	500	0.38	14.7
diethyl ether	0.251	512	0.43	14	516	0.32	12.4	516	0.37	14.9
ethyl acetate	0.292	586	0.02	2.3	588	0.02	1.9	589	0.03	2.9
tetrahydrofuran	0.308	586	0.05	2.5	588	0.02	1.5	596	0.04	3.7
dichloromethane	0.319	–	–	–	–	–	–	614	0.02	–
acetonitrile	0.393	–	–	–	–	–	–	685	< 0.01	–

[a] From Scherer[2a]. – [b] Second component of 3.4 ns observed.

occupied by the molecule in equation (2) ε_s is the solvent dielectric constant and *n* is its refractive index.

$$\nu_{CT} = \nu_{CT}(0) - \frac{2\mu_{CT}^2}{hc\rho^3}\Delta f = \nu_{CT}(0) - 10070\frac{\mu_{CT}^2}{\rho^3}\Delta f \quad (1)$$

$$\Delta f = \frac{(\varepsilon_s - 1)}{(2\varepsilon_s + 1)} - \frac{(n^2 - 1)}{(4n^2 + 2)} \quad (2)$$

The plots for the three compounds are given in Figure 2. The parameters obtained from the analysis are given in Table 2. Both the slopes and the intercepts are virtually identical for **1**−**3**. This implies that the energetics of the charge transfer state are not affected by the replacement of the cyano moiety by the ester moiety nor by the incorporation of the alkyl chain(s).

Table 2. Experimental parameters obtained [10^3 cm^{-1}] from the Lippert-Mataga analysis [equation (1)] of compounds **1**−**3**

Compound	$2\mu^2/hc\rho^3$	$\nu_{CT}(0)$
1	31.9	27.1
2	32.8	27.2
3	32.8	27.2

The fluorescence quantum yields of all three compounds are relatively high in nonpolar and moderately polar solvents. Nevertheless, in the alkane solvents the quantum yield of **3** is substantially higher than those of **1** and **2**, although the charge-separation distance and position of the charge-transfer state are nearly the same for the three compounds. The same trend is observed in the lifetimes. In the ether solvents the lifetimes of the charge-transfer states are virtually identical, whereas in the alkane solvents the lifetime of **3** is about twice as long as that of **1** and **2**. It has been observed before that the nonradiative decay rates of the CT states in compounds of this class are extremely sensitive to their energy, especially in the nonpolar alkane solvents.[8] A possibility is that in nonpolar media for compounds **1** and **2** mixing of the charge-transfer state with the locally excited state of the acceptor[9][10] is slightly more pronounced than for **3**. For **1** we can see the result of this mixing in an increase of the nonradiative rate constant (Table 3). For **2** in the alkane solvents a biexponential decay is observed, with only a small contribution (ca. 10%) of the component of 3.4 ns. No wavelength dependence is observed for the contribution of the lifetimes to the decay, indicating that the associated fluorescence spectra are completely overlapping. The biphasic decay is probably due to the presence of different conformers of the acceptor group, which differ slightly in their properties.

Figure 2. Lippert-Mataga plots for **1**, **2**, and **3** (see legend); the data for **2** and **3** are plotted with a vertical off-set of 2000 and 4000 cm^{-1}, respectively

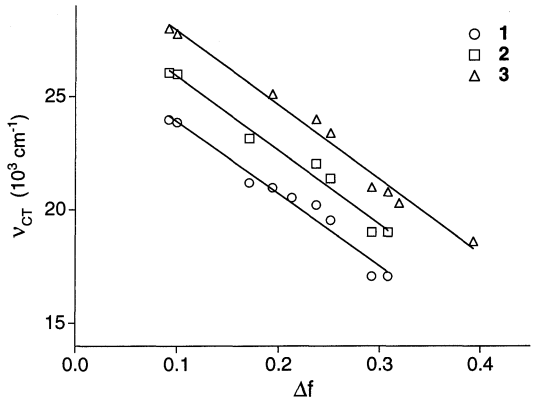

Fluorescence of 1a, 2a, and 3a

Steady-State Fluorescence

The fluorescence maxima and quantum yields of **1a**, **2a**, and **3a** measured in various solvents are given in Table 4. As for compounds **1**, **2**, and **3**, local fluorescence of the excited naphthalene chromophore is not detectable in the steady-state fluorescence spectra. Instead, also in these compounds solvatochromic charge-transfer fluorescence is observed. Especially in the nonpolar solvents the charge-transfer fluorescence maxima of compounds **1a**−**3a** are bathochromically shifted compared to the compounds with the exocyclic double bond **1**−**3**. The maxima observed for

Table 3. Radiative and nonradiative rate constants [10^6 s^{-1}] for compounds **1**−**3**

Solvent	Δf	**1**		**2**		**3**	
		k_f	k_d	k_f	k_d	k_f	k_d
n-hexane	0.092	132	395	–	–	115	94
cyclohexane	0.100	124	276	–	–	107	75
benzene	–	51	23	46	28	44	26
di-*n*-pentyl ether	0.171	52	32	60	29	–	–
di-*n*-butyl ether	0.194	49	34	–	–	34	33
di-*n*-propyl ether	0.213	43	40	–	–	–	–
diisopropyl ether	0.237	37	47	30	47	26	42
diethyl ether	0.251	31	41	26	55	25	42
ethyl acetate	0.292	9	426	11	516	10	334
tetrahydrofuran	0.308	20	380	13	653	11	259

1a−**3a** are in fact quite close to those of **4a**. This latter compound is known to undergo the harpooning process and in alkane solvents at room temperature only shows fluorescence originating from the CCT species in the steady-state fluorescence spectrum.

In the steady-state spectrum of the new compounds **1a**, **2a**, and **3a** in alkane solvents at room temperature we can, however, also observe a band at shorter wavelength (ca. 400 nm) next to the fluorescence band attributed to the CCT species (ca. 480 nm). The fluorescence spectra of **1a**, **2a**, and **3a** in *trans*-decalin are shown in Figure 3. From the excitation spectra, which are the same for detection at 400 and 480 nm, we can conclude that this short-wavelength emission is not originating from an impurity. The position of the band corresponds nicely to the expected fluorescence from the ECT species. In the older harpooning system **4a** such ECT fluorescence was not detectable at room temperature. These observations (Figure 3) strongly suggest that *the harpooning process is slowed down by the long alkyl tails*, especially when two tails are incorporated as in **1a**. Note that the cyano derivative **3a** has a higher fluorescence quantum yield than the two esters **1a** and **2a**, which is related to the more rapid nonradiative decay of the CCT species in the latter (vide infra).

Further information about the kinetic effect of the alkyl chains can be obtained by studying the temperature dependence of the fluorescence. The emission of compounds **1a**−**3a** in methylcyclohexane and in *trans*-decalin was studied as a function of the temperature. Some of the measured spectra of the three compounds in *trans*-decalin are shown in Figure 4, Figure 5, and Figure 6.

Figure 3. Steady-state fluorescence spectra of **1a**, **2a**, and **3a** in *trans*-decalin at room temperature, corrected for differences in absorbance at the excitation wavelength (308 nm)

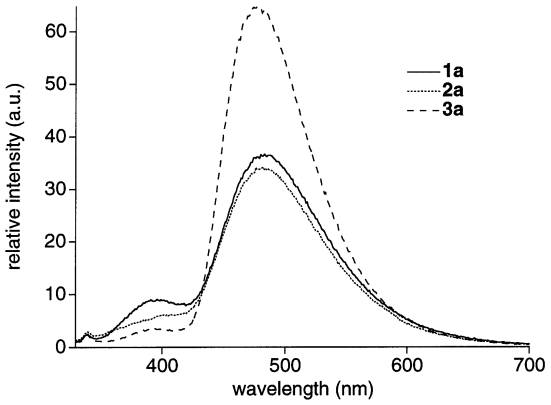

All compounds show an increase of the ECT emission upon lowering the temperature, concomitant with a decrease of the CCT emission. This must be caused by a decrease of the rate of interconversion of the two species. This effect is most pronounced for **1a**. At 173 K, e.g. the spectrum of **1a** (Figure 4) is dominated by the emission of the ECT species, whereas for **2a** (Figure 5) and **3a** (Figure 6) the intensities of the ECT and CCT emission are comparable.

Table 4. Charge-transfer fluorescence maxima [nm] and quantum yields for **1a**, **2a**, and **3a** (excitation wavelength 308 nm) in various solvents

Solvent	Δf	**1a**		**2a**		**3a**	
		λ_{max}	Φ_f	λ_{max}	Φ_f	λ_{max}	Φ_f
n-hexane	0.092	481	0.05	479	0.07	474	0.06
cyclohexane	0.100	482	0.08	481	0.07	476	0.13
trans-decalin	0.110	483	0.10	482	0.09	477	0.16
benzene	–	–	–	514	0.05	–	–
di-*n*-pentyl ether	0.171	497	0.05	498	0.05	497	0.08
diisopropyl ether	0.237	508	0.03	514	0.03	507	0.03
diethyl ether	0.251	522	0.02	522	0.03	521	0.03
ethyl acetate	0.292	596	< 0.01	592	< 0.01	600	< 0.01
tetrahydrofuran	0.308	–	–	598	< 0.01	598	< 0.01

Figure 4. Fluorescence spectra of **1a** in *trans*-decalin at various temperatures (excitation wavelength 308 nm)

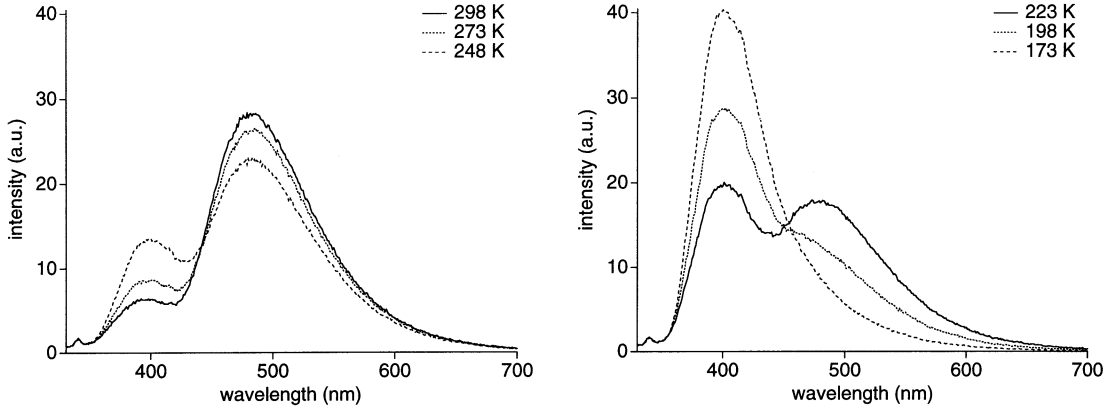

Figure 5. Fluorescence spectra of **2a** in *trans*-decalin at various temperatures (excitation wavelength 308 nm)

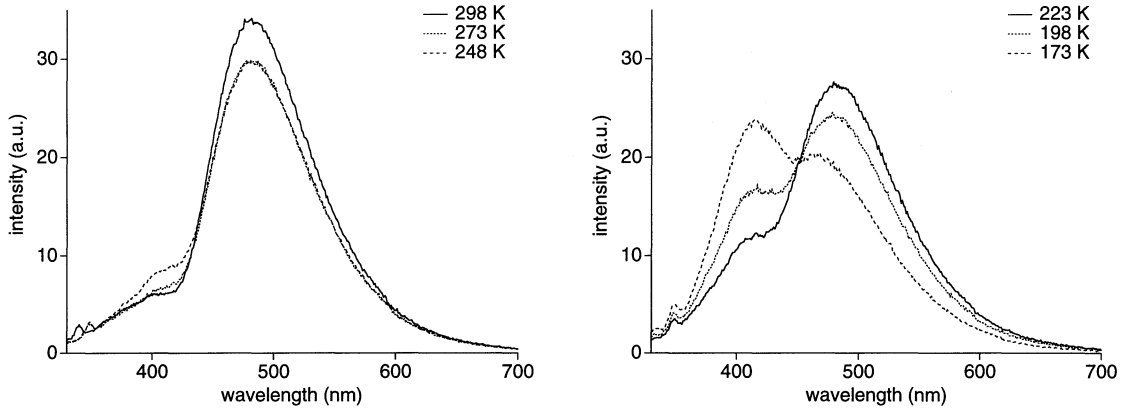

Figure 6. Fluorescence spectra of **3a** in *trans*-decalin at various temperatures (excitation wavelength 308 nm)

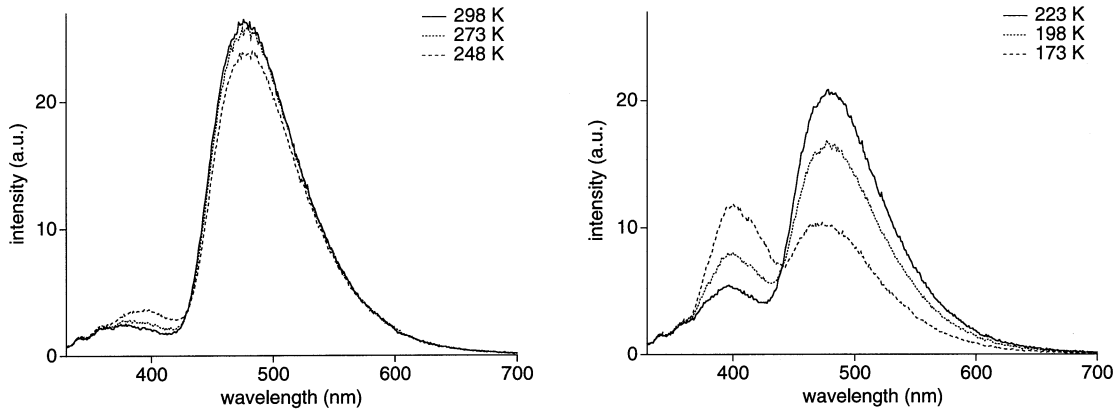

Although analysis of the temperature dependence of the fluorescence has often been used to determine activation barriers of intramolecular excimer and exciplex formation[11][12], it should be realized that variation of the temperature changes the properties of the solvent as well as those of the solute to a significant extent. Parameters like viscosity, dielectric constant and refractive index, which play vital roles in the solvating power (or polarity) of the solvent, are all affected by temperature. It is therefore practically impossible to separate the true effect of solvent viscosity from all others with these measurements and, as demonstrated earlier[3], only a combined temperature and pressure-dependent fluorescence study may be expected to provide reliable quantitative information on this aspect.

The fluorescence of the three new compounds and **4a** was also studied in Telene®, a saturated hydrocarbon polymer matrix. The emission spectrum was measured at 298 K as well as at 403 K, the latter being close to the glass transition temperature of Telene. The spectra of the four compounds are displayed in Figure 7. All compounds at 298 K show

Figure 7. Fluorescence spectra of **1a** (A), **2a** (B), **3a** (C), and **4a** (D) in a polymer matrix (Telene) at 298 K (full line) and 403 K (dashed line)

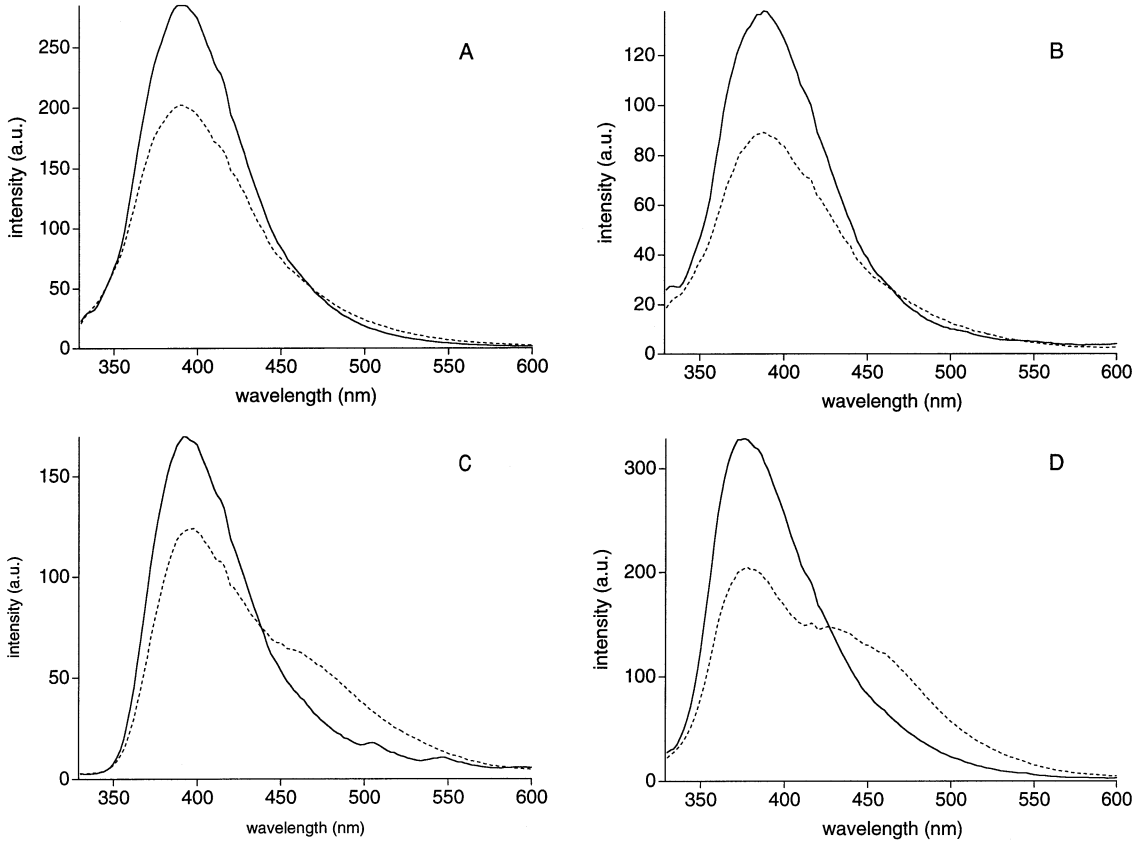

a single fluorescence band with a maximum close to that observed in nonpolar alkane solvents at low temperature. Thus, the folding process is effectively blocked in the rigid polymer matrix.

Upon heating the polymer sample, **3a** and **4a** clearly show the appearance of a new emission band at longer wavelength. When, after scaling, the spectra are subtracted the new fluorescence band is clearly visible. The maxima of the difference spectra are very close to those observed for the CCT species of these compounds in alkane solvents. For **1a** and **2a** hardly any changes in the shape of the spectra are observed upon heating. This is a quite interesting result because in solution as discussed above the barrier to folding appears to decrease in the order **1a** > **2a** ≈ **3a** > **4a**, while in the polymeric matrix this appears to be **1a** ≈ **2a** > **3a** > **4a**. Note that both **1a** and **2a** have a tetradecyl chain attached to the acceptor chromophore. It is expected that in the folding process, which requires a chair-boat conformational change, the part of the piperidine ring close to the acceptor will make the major translational motion to obtain the CCT state. As illustrated in Scheme 4, a compact CT state where donor and acceptor can form a true sandwich complex can be formed only by path B.

For **3a** at 298 K two additional narrow emission bands are observed at about 500 nm and 550 nm. This is attributed to phosphorescence of the cyanonaphthalene moiety.

Scheme 4. Schematic representation of the extended conformation and two of the possible compact conformers with the bridging piperidine moiety in a boat conformation

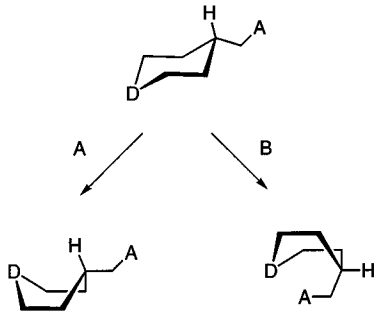

This phosphorescence is even more pronounced after heating and subsequent cooling of the polymer film under nitrogen. The triplet state must be populated from the ECT state because the initially prepared cyanonaphthalene singlet excited state undergoes quantitative charge separation, as indicated by the absence of "local" emission.

From the spectra at low temperature the maxima of the ECT emission can be determined in methylcyclohexane and *trans*-decalin. When the maxima, from Table 4 and those obtained from the low-temperature measurements, are plotted versus the corresponding solvent polarity parameters

(Δ), the Lippert-Mataga plots displayed in Figure 8 are obtained. The data can clearly not be fitted with single straight lines. Instead two linear regions can be observed.

Figure 8. Fluorescence maxima in various solvents of **1a** (A), **2a** (B), and **3a** (C) versus the corresponding Δf values; the data were fitted by two linear functions (see text); the maxima displayed by the filled symbols follow from fluorescence measurements at low temperature

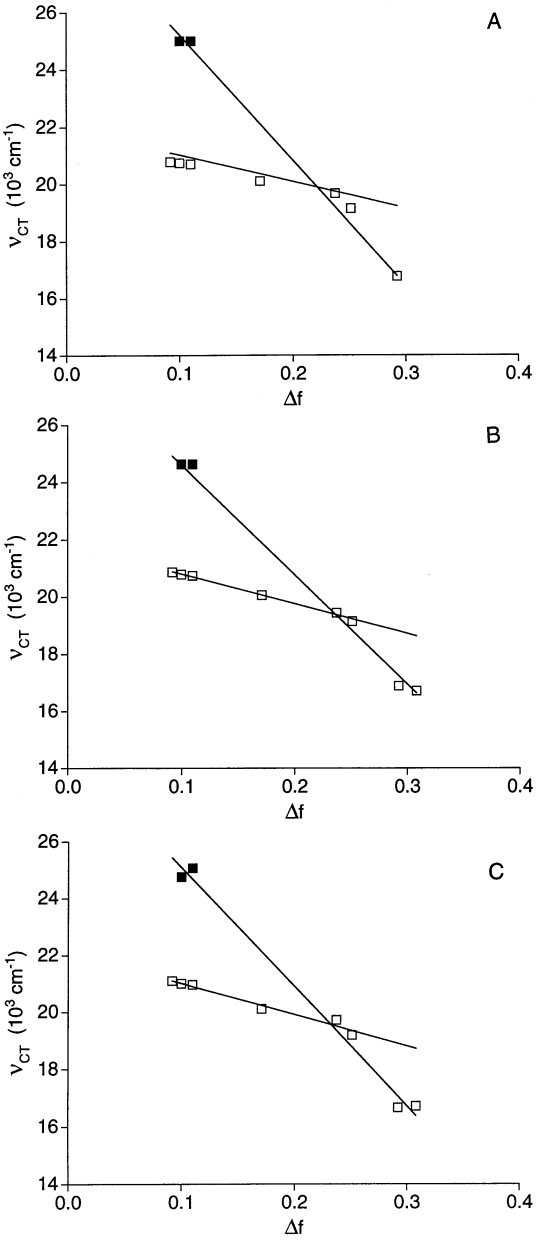

The experimental parameters, obtained by fitting the fluorescence maxima according to the Lippert-Mataga equation in the two regions, are given in Table 5. The smaller slopes (ca. $10{\cdot}10^3$ cm^{-1}) are reasonable values for a compact charge-transfer species. The slopes for the extended charge-transfer species (ca. $40{\cdot}10^3$ cm^{-1}) are comparable to the values Wegewijs found for **4a**. The crossing of the two linear fits occurs at a Δf value of about 0.23, close to that of diisopropyl ether (0.237). It is important to note that the applied analysis can only give a crude estimation of the dipole moments and a hint to in which solvents the folding process might still take place. One of the problems, especially in the medium-polarity region, is that we use the maxima of the steady-state fluorescence spectra. If harpooning occurs, e.g. in di-*n*-pentyl ether, the maximum used in fact is the average of the now strongly overlapping ECT and CCT emissions. To obtain the fluorescence maxima of the true ECT and CCT species in a solvent where the folding process takes place, the only experimental approach which appears feasible is to reconstruct the species-associated spectra from decay curves at multiple wavelengths. This is, however, a rather time-consuming experiment. In the next section we will study the fluorescence decay at a limited number of wavelengths to obtain an indication in which solvents the studied compounds still undergo the folding process.

Table 5. Experimental parameters [10^3 cm^{-1}] for **1a**−**3a** obtained from Lippert-Mataga analysis (equation 1)

Compound	ECT		CCT	
	$2\mu^2/hc\rho^3$	$\nu_{CT}(0)$	$2\mu^2/hc\rho^3$	$\nu_{CT}(0)$
1a	43.9	29.6	9.3	21.7
2a	38.3	28.4	10.4	21.8
3a	41.9	29.3	11.1	22.1

Time-Resolved Fluorescence, Single-Photon Counting

In *trans*-decalin and cyclohexane solutions the fluorescence decay was measured at about 14 wavelengths between 370 and 600 nm and with different time windows. All time profiles could be fitted with two major components. For **1a** and **2a** a third short component was observed at short wavelengths (< 370 nm). This either is some residual local fluorescence of the acceptor chromophore or an impurity. As the contribution of this component was only minor we disregard it in the following discussion. Global analysis of the time profiles was performed for two wavelength regions, between 370 and 430 nm and between 450 and 600 nm. In the short-wavelength region the time profiles are dominated by a decaying component, which we attribute to the ECT species, fluorescing at about 400 nm. In the other region we observe a biexponential time profile: a rising component with a similar time constant as the decay time at short wavelength and a much more slowly decaying component. We attribute this biexponential decay to fluorescence from the CCT species, which has its fluorescence maximum around 480 nm. As expected the decay time at short wavelength is virtually identical to the rise time observed at longer wavelength, supporting the view that the extended charge-transfer species is the precursor of the folded charge-transfer species. The fitted decay and rise times in methylcyclohexane and *trans*-decalin are given in Table 6.

In methylcyclohexane the rise time of **4a** is significantly shorter than those of **1a**, **2a**, and **3a**. The ECT decay and CCT rise times of **2a** and **3a** are similar in magnitude, but

Table 6. Rise and decay times [ns] of the fluorescence of **1a**, **2a**, **3a**, and **4a** in methylcyclohexane and *trans*-decalin at room temperature (the ECT decay was monitored below 440 nm, the CCT decay at wavelengths larger than 440 nm)

	Methylcyclohexane			*trans*-Decalin		
	ECT	CCT		ECT	CCT	
Compound	τ_{decay}	τ_{rise}	τ_{decay}	τ_{decay}	τ_{rise}	τ_{decay}
1a	2.5	3.0	26	6.6	6.6	30
2a	2.0	1.7	26	3.1	4.0	23
3a	1.1	1.1	44	3.4	3.2	42
4a	–	0.5[a]	54[b]	2.0	–	61[a]

[a] From Wegewijs[1a]. – [b] From Jäger et al.[3]

those of **1a** are significantly longer, showing that the introduction of two tetradecyl chains has a much larger impact on the folding process than merely introducing a single tetradecyl chain. From the results it clearly follows that the introduction of the tetradecyl chains has a substantial influence on the folding process. Note that the decay of the ECT species at room temperature is strongly dominated by the folding process so that the interconversion rate ECT → CCT follows almost directly from the observed time constant. When the interconversion is hampered by a solid medium or at low temperature strong ECT emission can be observed in all four compounds. For the CCT species the lifetime of **3a** is considerably longer than those of **1a** and **2a**, which contributes to the relatively high fluorescence quantum yield (Table 4).

The fluorescence decay of the three compounds was also studied in benzene, di-*n*-pentyl ether, diisopropyl ether, diethyl ether, ethyl acetate, and tetrahydrofuran at about 5 wavelengths (Table 7). In benzene, di-*n*-pentyl ether, and diethyl ether a clear rise was observed at the red side of the fluorescence band, in addition to a slower decaying component. The rise and decay times were fitted by global analysis. For the extended charge-transfer species, we expected a corresponding decay time at shorter wavelength, but this could in most solvents not be resolved properly. The biphasic time profile, however, indicates that even in these relatively polar solvents the compounds still undergo a conformational change as was already indicated by the Lippert-Mataga plots (Figure 8). The decay of the charge transfer fluorescence, measured for **2a** and **3a** in diisopropyl ether, could be reasonably well fitted with a single component. For **1a** and **2a** in ethyl acetate and tetrahydrofuran also two components were observed, with the shortest contributing only little. These are, however, two independently decaying species. A likely explanation is the presence of two different conformers, as was already suggested for the corresponding systems **1** and **2**.

The time-resolved measurements thus indicate that even in relatively polar solvents, like diethyl ether, the compounds still undergo a conformational change. The results presented above, however, are not considered conclusive evidence for this hypothesis. We are currently studying the fluorescence of the three new compounds and **4a**, the first compound in which the harpooning process was observed, in a time-resolved fashion with a streak camera. The powerful combination of two-dimensional photon counting using a streak camera and the application of a spectrotemporal parametrization method will allow us to investigate the harpooning process in much more detail. The results of these studies will be reported separately.

Table 7. Rise and decay times [ns] of the charge-transfer fluorescence of **1a**–**3a**, measured with single-photon counting; the decay was monitored at about 5 wavelengths and the traces were fitted by global analysis; the rise is observed on the long-wavelength side of the emission band (ECT)

Solvent	**1a**		**2a**		**3a**	
	τ_{rise}	τ_{decay}	τ_{rise}	τ_{decay}	τ_{rise}	τ_{decay}
benzene	6.2	26.7	–	–	5.2	20.8
di-*n*-pentyl ether	12.4	27.2	8.7	23.4	8.4	29.2
diisopropyl ether	–	–	–	10.2	–	18.4
diethyl ether	7.3	24.8	5.0	14.9	5.5	18.6
ethylacetate	–	9.6 (95%) 2.0 (5%)	–	6.3 (83%) 1.4 (17%)	–	17.0
tetrahydrofuran	–	15.3 (97%) 2.5 (3%)	–	9.8 (84%) 1.8 (16%)	–	23.6

Time-Resolved Microwave Conductivity Measurements

The time-resolved microwave conductivity (TRMC) technique has proven its value over the years for the study of donor-acceptor compounds[13]. It is based on the change in the microwave power reflected by a microwave cavity on flash photolysis of a solution within the cavity. From this change the change in microwave conductivity (dielectric loss) can be determined. In the case of donor-acceptor molecules, this change in conductivity is caused by the increased dipole moment, μ_{CT}, of the solute as a consequence of photoinduced charge transfer. The change in conductivity is related to the concentration of the excited molecules, N^*, and the dipole moments of the ground and excited states, μ_0 and μ_*, respectively, by equation (3). In equation (3) k_B is the Boltzmann constant, T is the temperature and ε_∞ is the high-frequency dielectric constant of the solution, equal to the square of the refractive index for nonpolar solvents; ΔZ, the excess polarity of the excited state is given by equation (4).

$$\Delta\sigma = \frac{(\varepsilon_\infty + 2)^2}{27 k_B T} \cdot N^* \cdot \Delta Z \qquad (3)$$

$$\Delta Z = \left(\frac{\mu_*^2 \cdot F(\omega\Theta_*)}{\Theta_*} - \frac{\mu_0^2 \cdot F(\omega\Theta_0)}{\Theta_0} \right) \qquad (4)$$

In equations (3) and (4), Θ_0 and Θ_* are the dipole relaxation times of the ground and excited states, respectively. $F(\omega\Theta)$ in (4) is the dispersion parameter which for a Debye-

type relaxation is given by equation (5), where ω (= 2πν) is the radian frequency of the microwaves (ν ≈ 10 GHz).

$$F(\omega\Theta) = \frac{(\omega\Theta)^2}{1+(\omega\Theta)^2} \quad (5)$$

The concentration of excited molecules is calculated from the incident intensity of the laser pulse, the optical density of the solution, and the kinetic parameters governing the formation and decay of the intermediates formed subsequent to photoexcitation as described previously[14][15]. By fitting the calculated time dependence of the concentration of the intermediates to the conductivity transients observed, the product of quantum yield for a particular intermediate and its excess polarity, $\phi_n\Delta Z_n$, can be determined.

In many cases ΔZ_n can be simplified. For example, if the dipole relaxation time is longer than about 75 ps (as is the case for the present compounds), $F(\omega\Theta)$ will be within 5% of unity. Of the compounds studied, the excited-state dipole moments are generally more than an order of magnitude larger than those of the ground state. Under these conditions the second term in equation (4) can be neglected. The parameter determined from the fitting procedure can therefore to a good approximation be described by equation (6).

$$\phi_n\Delta Z \approx \phi_n\left[\frac{\mu_n^2}{\Theta_n} - \frac{\mu_0^2}{\Theta_0}\right] \approx \phi_n\frac{\mu_n^2}{\Theta_n} \quad (6)$$

The compounds **1**, **2**, **3**, **1a**, **2a**, and **3a** together with **4** and **4a** were studied by flash-photolysis time-resolved microwave conductivity (TRMC) in the relatively viscous solvent *trans*-decalin at room temperature. The conductivity transients for the rigidly bridged systems (**1**, **2**, **3**, and **4**) (Figure 9, left column) could be satisfactorily fitted with the major component being identical in decay time to the fluorescence decay (τ_{fl}). However, a small, more slowly decaying component was necessary in order to fit the conductivity transients at longer times. The values of $\phi_1\Delta Z_1$ and $\phi_2\Delta Z_2$ and the lifetimes determined for the two components are listed in Table 8. As can be seen, τ_2 is approximately an order of magnitude larger than τ_1. From fluorescence studies no evidence was found for such a long-lived transient. As the relative contribution of this component is small, we concentrated on the first component. Because of the lack of local emission of the initially excited acceptor chromophore (vide supra), we can conclude that the ECT species is formed with close to unit efficiency, i.e. $\phi_1 \approx 1$. The dipole moment of this species can therefore be determined from $\phi_1\Delta Z_1$ according to equation (6) if the dipole relaxation time Θ_1 is known. The dipole relaxation times will be determined by rotational diffusion and we have calculated the rotational relaxation times on the basis of the molecular weights assuming as a first approximation a cylindrical geometry, as described previously[15]. The calculated values of Θ are listed in Table 8. These have been used to make estimates of the given excited state dipole moments (μ_1). The value of 33 D found for **4** is in good agreement with a previous value of 31 D determined for cyclohexane as solvent[6a].

The dipole moment estimates for the other compounds with the tetradecyl group(s) attached to the chromophore(s) are seen to be much larger than that of **4** itself. Since the basic donor-acceptor geometry is expected to be virtually unchanged by the introduction of the alkyl tails, a larger excited state dipole moment would not be expected. The reason for the discrepancy must be the conformational freedom of the tetradecyl chains, which makes the approximation of a rigid cylindrical geometry no longer suitable for deriving the rotational relaxation time. If we make the assumption that the excited state dipole moment is the same for all of the compounds (as we concluded earlier from the solvatochromic shifts, vide supra), and equal to that determined for **4**, then we can use the ΔZ_1 values of **4** to derive the actual rotational relaxation time of the tetradecyl-substituted molecules from equation (7).

$$\Theta = \frac{\Delta Z_{EP}}{\Delta Z}\cdot\Theta_{FP} \quad (7)$$

The values obtained using this formula are listed in Table 8. While these values of Θ are considerably smaller than those calculated based on a rigid cylindrical geometry, they are still substantially larger than the values calculated for a spherical shape which are listed as Θ_{sph} in Table 8.

For the semiflexibly bridged systems **4a**, **1a**, **2a**, and **3a**, it was impossible to obtain even a moderately good fit using a single-component analysis with the fluorescence lifetimes. Using a two component fitting procedure, with the values of τ_1 and τ_2 almost identical to the ECT and CCT fluorescence decay times, satisfactory fits were obtained as shown in the right-hand part of Figure 10. The calculated values of $\phi_1\Delta Z_1$ and $\phi_2\Delta Z_2$ are listed in Table 9.

Since the first dipolar excited state is expected to have an extended geometry similar to that for the rigidly bridged systems, we have used the values of Θ estimated for the latter compounds to derive values of the dipole moments from the $\phi_1\Delta Z_1$ values assuming ϕ_1 to be close to unity. The values obtained are seen to be somewhat larger than the 33 D found for **4**, which can be explained by the slight increase in donor−acceptor distance upon hydrogenation of the exocyclic double bond. Only the dipole moment of **2a** appears somewhat lower than that of the other compounds for reasons that we do not understand.

From the temperature dependence of the fluorescence of the ECT state for **4a**[1c][1g] it can be estimated that at room temperature the quantum yield for formation of the second dipolar state is approximately 95%. Using this value together with the measured value of $\phi_2\Delta Z_2$ and the value of Θ = 653 ps, corresponding to an extended, cylindrical geometry, would result in an estimated dipole moment of 22 D. This is in accordance with the second charge-transfer species being in fact a folded conformer of the first. In this case an estimate of the rotational relaxation time based on a spherical model may be more appropriate. If this is used the rotational relaxation time is reduced from 653 ps to 236 ps. The value of the dipole moment calculated is corre-

Figure 9. TRMC transients (dots) with fits (solid line) and both components of the fit (dotted and dashed successively) of the rigidly bridged compounds (left column) and the semiflexibly bridged compounds (right column) in *trans*-decalin at room temperature

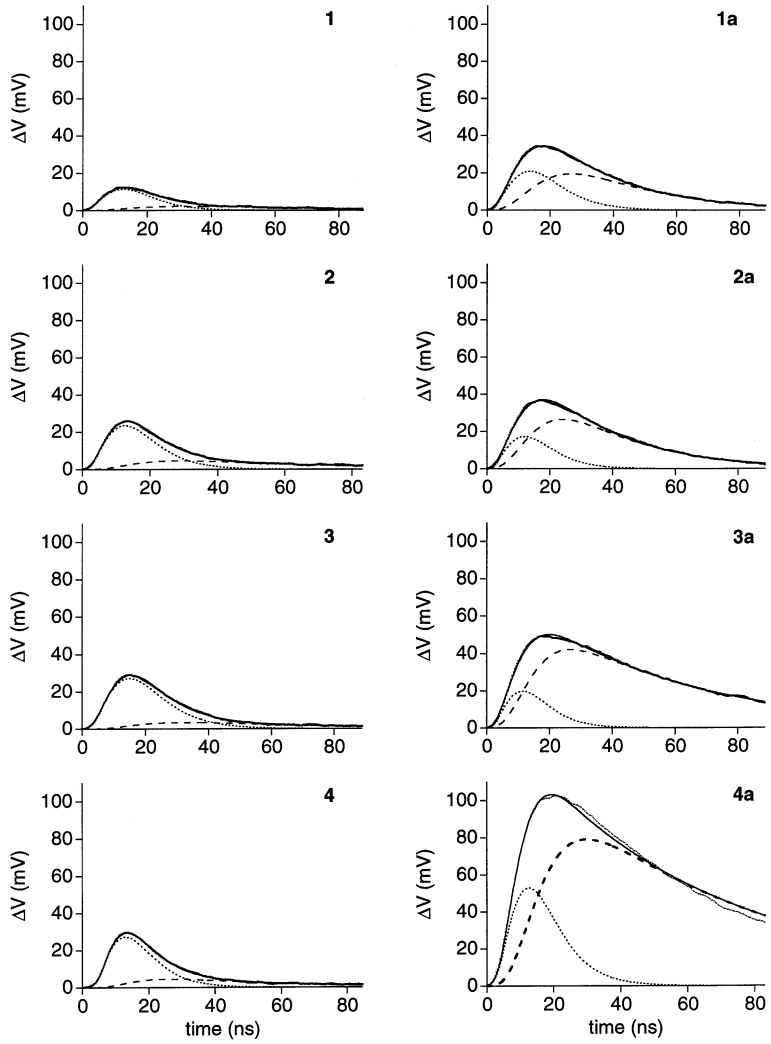

Table 8. Fit parameters for the TRMC transients of the rigidly bridged systems **1**, **2**, **3**, and **4** in *trans*-decalin at room temperature

Compound	τ_1 [ns][a]	$\phi_1\Delta Z_1$ [D^2 ps^{-1}]	τ_2 [ns][b]	$\phi_2\Delta Z_2$ [D^2 ps^{-1}]	Θ_{cyl} [ps]	μ_1 [D][c]	Θ_1 [ps][d]	Θ_{sph} [ps]
1	4.6	0.439	62	0.028	4818	46	2435	533
2	3.6	0.789	46	0.039	2352	43	1354	401
3	7.8	0.703	43	0.046	2020	38	1521	377
4	1.8	1.637	34	0.042	653	33	–	235

[a] From fluorescence decay. – [b] from the fit to the conductivity decay at longer times. – [c] By using $\Theta_1 = \Theta_{cyl}$. – [d] By assuming μ_1 = 33 D.

spondingly reduced to circa 13 D. This value is close to the dipole moments found for intermolecular donor-acceptor exciplexes which have a face-to-face distance of about 3.4 Å. We conclude that the actual dipole moment of the folded form of **4a** lies somewhere between the values of 13 D and 22 D derived on the basis of a spherical or cylindrical geometry. Assuming an identical quantum yield for formation of the CCT state (ϕ = 0.95) for the other compounds and using the rotational relaxation times listed in Table 8, we calculated the dipole moments for the CCT state listed in the last and second last column. As for **4a** these are again considerably smaller than those of the ECT state.

Concluding Remarks

We have presented the synthesis of six new donor-acceptor compounds which contain a long tetradecyl chain connected to either the donor or acceptor moiety or both of them. The systems **1**, **2**, and **3**, all analogs of the fluorescent probe

Table 9. Fit parameters for the TRMC transients of the semiflexibly bridged systems **1a**, **2a**, **3a**, and **4a** in *trans*-decalin

Compound	τ_1 [ns][a]	$\phi_1\Delta Z_1$ [D^2 ps^{-1}]	τ_2 [ns][a]	$\phi_2\Delta Z_2$ [D^2 ps^{-1}]	μ_1 [D][b]	μ_2 [D][c]	μ_2 [D][d]
1a	6.6	0.575	25	0.313	38	28	13
2a	4.0	0.648	25	0.400	30	24	13
3a	3.2	0.993	50	0.525	39	29	14
4a	2.0	2.59	61	0.722	41	22	13

[a] From fluorescence decay. – [b] By using the values of Θ_1 from Table 8. – [c] By using $\phi_2 = 0.95$ and $\Theta_2 = \Theta_1$ from Table 8. – [d] By using $\phi_2 = 0.95$ and $\Theta_2 = \Theta_{sph}$ from Table 8.

molecule Fluoroprobe, show relatively strong charge-transfer fluorescence in solvents of low and medium polarity. From the charge-transfer fluorescence maxima it can be concluded that the ester moiety, present in **1** and **2** is equally electron-withdrawing as the cyano substituent in **3**.

The systems **1a**, **2a**, and **3a**, obtained after hydrogenation of the exocyclic double bond of **1**, **2**, and **3**, respectively, all undergo the photoinduced harpooning process in nonpolar and probably also in medium polarity solvents. As the electron-accepting properties of the naphthalene acceptor units are virtually identical, a fair comparison between the different compounds can be made. Both the steady-state fluorescence spectra and the decay times of the ECT and CCT species show that the photoinduced folding process can be effectively slowed down by the introduction of the long alkyl tails. This is most pronounced for **1a** which has the tetradecyl group attached to both donor and acceptor. The difference in the rate of folding between **2a** and **3a**, having an *n*-tetradecyl chain attached only to the acceptor and donor, respectively, is relatively small in liquid solution. Flash-photolysis microwave-conductivity measurements give additional evidence for the presence of the ECT → CCT conversion in the viscous solvent *trans*-decalin.

Ing. *D. Bebelaar* is gratefully acknowledged for technical assistance with the SPC measurements, *M. Koeberg* for help with some of the experiments and *G. W. Buning (Philips Research Laboratories)* for the generous gift of Telene. This research was supported (in part) by *The Netherlands Foundation for Chemical Research (SON)* with financial aid from *The Netherlands Organization for the Advancement of Research (NWO)*.

Experimental Section

Measurements: Telene OP 2000x (BFGoodrich Company) is a hydrocarbon polymer consisting of bicyclo[2.2.1]heptane units. The polymer films were prepared by dissolving the polymer beads and a small amount of the donor-acceptor compound in spectrograde toluene (Aldrich). After evaporation of the solvent (at ambient temperature and pressure), the polymer films were dried in a vacuum desiccator.

Electronic absorption measurements were performed with a Hewlett-Packard 8453 diode-array spectrometer. Molar absorption coefficients were determined using concentrations of 10^{-4}–10^{-5} M. Commercially available spectrograde solvents were used.

Fluorescence spectra were recorded with a Spex Fluorolog II emission spectrometer using an RCA-C31034 GaAs photomultiplier as the detector. Spectra were corrected for the wavelength-dependent response of the detection system. Fluorescence quantum yields were determined relative to a reference solution [quinine bisulfate in 1 N sulfuric acid ($\phi = 0.546$)[17]] and corrected for the refractive index of the solvent. The samples were made with an absorbance between 0.1 and 0.2 (in 1 cm) at the excitation wavelength and were deoxygenated by purging with argon for 15 min. Commercially available spectrograde solvents were used (Merck, Uvasol), except for di-*n*-butyl ether (Merck, > 99%, washed three times with sulfuric acid). When the purity of the solvent was found to be insufficient, the solvent was purified by standard procedures[18]. All alkyl ethers were distilled from CaH_2 or $LiAlH_4$ prior to use. Ethyl acetate was washed with a saturated sodium carbonate solution and distilled from CaH_2. Fluorescence measurements at low temperature were performed using an Oxford Instruments liquid-nitrogen cryostat DN 1704 with an ITC4 control unit. The samples were degassed by at least four freeze-pump-thaw cycles. Each sample was allowed to thermally equilibrate for at least 20 min prior to data collection.

Fluorescence decay curves were measured by means of picosecond time-correlated single-photon counting (SPC). The experimental set-up has been fully described elsewhere[19]. A mode-locked argon-ion laser (Coherent 486 AS Mode Locker and Coherent Innova 200 laser) was used to pump synchronously a DCM dye-laser (Coherent model 700). The output frequency was doubled with a BBO crystal resulting in 310–320 nm pulses. A Hamamatsu microchannel plate photomultiplier (R3809) was used as detector. The response function (*fwhm* ≈ 18 ps) was obtained by monitoring at the Raman band of a cell filled with spectrograde water. The cells were painted black with camera varnish on two adjacent sides to avoid reflection at the quartz/air boundary. The decay traces were deconvoluted with a computer program using non-linear least-squares fitting[20].

Solutions for TRMC measurements were prepared in purified *trans*-decalin with an absorbance at 308 nm of 1 in 1 cm. The solution was purged with CO_2 to remove air and scavenge free electrons that might be generated by low-yield photoionization processes. The sample was contained in a microwave cavity and irradiated with a 308 nm pulse (7 ns FWHM) of a Lumonics HyperEx 400 excimer laser. Transients were measured at the resonance frequency. To improve the signal-to-noise ratio up to 64 transients were averaged. To quantify the results, a solution of 4-(*N,N*-dimethylamino)-4′-nitrostilbene (DMANS) was used as an internal actinometer. The relevant equations for the data analysis have been given together with the results (vide supra). The microwave circuitry, its operation, and the procedure of the data analysis have been fully described elsewhere[14].

NMR spectra were measured with a Bruker ARX-400 (400 MHz and 100 MHz, for ^1H and ^{13}C, respectively) or Bruker AC-200 (200 MHz and 50 MHz, for ^1H and ^{13}C, respectively).

1-(4-Tetradecylphenyl)piperidin-4-one: A solution of 1,5-dichloro-3-pentanone (2.33 g, 15 mmol) and a solution of 4-tetradecylaniline (4.34 g, 15 mmol), both in 40 ml of methanol, were simultaneously added to a refluxing slurry of sodium carbonate (3.82 g, 36 mmol) in 15 ml of methanol over a period of about 20 min. After the addition of the two solutions, the reaction mixture was heated at reflux temperature for 1.5 h. After cooling to room temperature, the reaction mixture was concentrated and water (ca. 30 ml) was added. After extraction with $CHCl_3$ (3 × 30 ml), the combined extracts were dried with magnesium sulfate, filtered, and concentrated to give a brown solid. The product was purified by column chromatography on neutral alumina with petroleum ether 40−65/diethyl ether (1:1), yielding a light-brown solid (2.30 g, 41%). − ^{1}H NMR (400 MHz, $CDCl_3$): δ = 7.11 (d, *J* = 9.0 Hz, 2 H), 6.91 (d, *J* = 9.0 Hz, 2 H), 3.56 (t, *J* = 6 Hz, 4 H), 2.51−2.58 (m, 6 H), 1.58−1.65 (m, 2 H), 1.26 (br. s, 22 H), 0.88 (t, *J* = 7 Hz, 3 H).

1-(p-Tolyl)-4-piperidin-4-one: The compound was synthesized as described for 1-(4-tetradecylphenyl)piperidin-4-one on a 21.0-mmol scale. After column chromatography, 1-(*p*-tolyl)-4-piperidin-4-one was obtained as an orange solid (1.98 g, 49%) and was used without further purification. − ^{1}H NMR (400 MHz, $CDCl_3$), δ = 7.11 (d, *J* = 8.4 Hz, 2 H), 6.93 (d, *J* = 8.4 Hz, 2 H), 3.55 (t, *J* = 6.0 Hz, 4 H), 2.57 (t, *J* = 5.9 Hz, 4 H), 2.29 (s, 3 H).

4-Methylnaphthalene-1-carboxylic Acid: 1-Bromo-4-methylnaphthalene (25 g, 0.113 mol) in dry diethyl ether (45 ml) was added dropwise to magnesium granules (3 g, 0.123 mol). The reaction mixture was stirred for 2 h and poured onto powdered CO_2 (30 g, 0.68 mol). After the addition of water (50 ml) and diethyl ether (100 ml), the mixture was acidified with sulfuric acid, and the ether layer was separated. The water layer was extracted with diethyl ether and the collected ether layers were extracted with a 2 N NaOH solution (2 × 100 ml). The solution was acidified with sulfuric acid and extracted with diethyl ether. After drying with sodium sulfate and concentration, 4-methylnaphthalene-1-carboxylic acid was obtained as a brown solid (5.33 g, 25%). − ^{1}H NMR (400 MHz, $CDCl_3$), δ = 8.96 (m, 1 H), 8.13 (m, 1 H), 8.07 (d, *J* = 7.4 Hz, 1 H), 7.60−7.71 (m, 2 H), 7.47 (d, *J* = 7.4 Hz, 1 H), 2.73 (s, 3 H).

Tetradecyl 4-Methylnaphthalene-1-carboxylate: First, 4-methylnaphthalene-1-carbonyl chloride was prepared by heating at reflux temperature 4-methylnaphthalene-1-carboxylic acid (5.3 g, 28.6 mmol) in $SOCl_2$ (20 ml). The excess $SOCl_2$ was removed by distillation after addition of toluene. The obtained solid (5.85 g) was dissolved in toluene (40 ml), and tetradecanol (5.70 g, 26.5 mmol) in toluene (20 ml) was added dropwise. After 30 min, pyridine (2.1 g, 26.5 mmol) was added. The reaction mixture was stirred overnight and water (40 ml) and CH_2Cl_2 (50 ml) were added. The water layer was separated and extracted with CH_2Cl_2. The combined organic layers were dried with sodium sulfate, filtered and the solvent was evaporated to give a brown solid. The product was purified by column chromatography on silica with CH_2Cl_2 (yield 9.22 g, 91%). − ^{1}H NMR (400 MHz, $CDCl_3$), δ = 8.98 (m, 1 H), 8.1 (m, 2 H), 7.55−7.64 (m, 2 H), 7.35 (d, *J* = 7.4 Hz, 1 H), 4.40 (t, *J* = 6.7 Hz, 2 H), 2.75 (s, 3 H), 1.83 (m, 2 H), 1.49 (m, 2 H), 1.26−1.41 (m, 20 H), 0.89 (t, *J* = 7 Hz, 3 H).

Tetradecyl 4-Bromomethylnaphthalene-1-carboxylate: Tetradecyl 4-methylnaphthalene-1-carboxylate (5.74 g, 15 mmol) and NBS (2.85 g, 16 mmol) were dissolved in CCl_4. A catalytic amount of dibenzoyl peroxide was added and the reaction mixture was heated at reflux temperature for 3 h. NMR analysis showed that only about 40% of the desired product was formed. More NBS (1.68 g, 9.4 mmol) was added and the reaction mixture was was heated at reflux temperature for an additional 2 h. After cooling to room temperature, the reaction mixture was filtered through a glass filter and the solvent was evaporated. The obtained solid was recrystallized from petroleum ether 40−65, yielding orange crystals (5.17 g, 75%). − ^{1}H NMR (400 MHz, $CDCl_3$), δ = 8.93 (m, 1 H), 8.20 (m, 1 H), 8.06 (d, *J* = 7.4 Hz, 1 H), 7.62−7.70 (m, 2 H), 7.57 (d, *J* = 7.5 Hz, 1 H), 4.95 (s, 2 H), 4.41 (t, *J* = 6.7 Hz, 2 H), 1.82 (m, 2 H), 1.49 (m, 2 H), 1.25−1.44 (m, 20 H), 0.88 (t, *J* = 7 Hz, 3 H).

Tetradecyl 4-(Diethoxyphosphorylmethylnaphthalene-1-carboxylate: The compound was obtained by heating tetradecyl 4-bromomethylnaphthalene-1-carboxylate (2.50 g, 5.42 mmol) in triethyl phosphite (3 g, 18.1 mmol) at 90°C for 3 h. The excess triethyl phosphite was removed under reduced pressure and the crude product was recrystallized from petroleum ether 40−65, yielding off-white crystals (2.49 g, 89%). − ^{1}H NMR (400 MHz, $CDCl_3$), δ = 8.94 (m, 1 H), 8.16 (m, 1 H), 8.10 (d, *J* = 7.5 Hz, 1 H), 7.58−7.62 (m, 2 H), 7.51 (dd, *J* = 7.4/3.5 Hz, 1 H), 4.40 (t, *J* = 6.7 Hz, 2 H), 3.90−4.0 (m, 4 H), 3.68 (d, *J* = 22.5 Hz, 2 H), 1.82 (m, 2 H), 1.48 (m, 2 H), 1.25−1.39 (m, 20 H), 1.16 (t, *J* = 7.1 Hz, 6 H), 0.88 (t, *J* = 7 Hz, 3 H).

Tetradecyl 4-[1-(4-Tetradecylphenyl)piperidin-4-ylidenemethyl]-naphthalene-1-carboxylate (**1**): 1-(4-Tetradecyl-phenyl)-piperidin-4-one (0.51 g, 1.37 mmol) and tetradecyl 4-(diethoxyphosphorylmethyl)naphthalene-1-carboxylate (0.75 g, 1.37 mmol) were dissolved in dry THF. NaH (140 mg, 3.2 mmol) (55−60% suspension in paraffin oil) was added in portions. The reaction mixture was heated for 4 h at 40°C, after which the reaction mixture was poured into water and extracted with petroleum ether 40−65. The crude product was purified by column chromatography on silica gel with $CHCl_3$/acetone (10:1). A small amount was crystallized from petroleum ether, yielding off-white crystals (0.758 g, 75%), m.p. 72°C. − ^{1}H NMR (400 MHz, $CDCl_3$), δ = 8.95 (m, 1 H), 8.13 (m, 1 H), 8.09 (d, *J* = 8.2 Hz, 1 H), 7.53−7.62 (m, 2 H), 7.32 (d, *J* = 7.5 Hz, 1 H), 7.08 (d, *J* = 7.8 Hz, 2 H), 6.9 (br. s, 2 H), 6.75 (s, 1 H), 4.41 (t, *J* = 6.7 Hz, 2 H), 3.38 (br. s, 2 H), 3.14 (br. s, 2 H), 2.66 (br. s, 2 H), 2.52 (t, *J* = 7.7 Hz, 2 H), 1.83 (m, 2 H), 1.6−1.2 (m, 48 H), 0.9 ('t', 6 H). − $C_{51}H_{77}NO_2$ (736.2): calcd. C 83.21, H 10.54, N 1.90; found C 83.05, H 10.41, N 1.78.

Tetradecyl 4-[1-(4-Tetradecylphenyl)piperidin-4-ylmethyl]naphthalene-1-carboxylate (**1a**): Compound **1** (200 mg, 0.27 mmol) in petroleum ether 40−65 was hydrogenated at 50 psi in a Parr apparatus for about 72 h in the presence of Pd (10% on carbon). The catalyst was filtered off and the solvent was evaporated. The obtained white solid was purified by column chromatography on silica gel with CH_2Cl_2 and recrystallization from petroleum ether 40−65, yielding white plates (104 mg, 52%), m.p. 77°C. − ^{1}H NMR (400 MHz, $CDCl_3$), δ =: 8.97 (m, 1 H), 8.09 (m, 2 H), 7.63−7.55 (m, 2 H), 7.33 (d, *J* = 7.5 Hz, 1 H), 7.05 (d, *J* = 8.3 Hz, 2 H), 6.85 (d, *J* = 8.1 Hz, 2 H), 4.40 (t, *J* = 6.7 Hz, 2 H), 3.60 (br. d, *J* = 8.2 Hz, 2 H), 3.08 (d, *J* = 6.9 Hz, 2 H), 2.5 (m, 4 H), 1.80 (m, 5 H), 1.6−1.1 (m, 48 H), 0.83 ('t', *J* = 7 Hz, 6 H). − $C_{51}H_{79}NO_2$ (738.2) : calcd. C 82.98, H 10.79, N 1.90; found C 83.15, H 10.79, N 1.80.

Tetradecyl 4-(1-p-Tolylpiperidin-4-ylidenemethyl)naphthalene-1-carboxylate (**2**): The compound was synthesized as described for **1**, with 1-*p*-tolyl-4-piperidin-4-one (0.37 g, 1.95 mmol). Purification was performed by column chromatography on silica gel with CH_2Cl_2 and recrystallization from pentane, yielding **2** as light-yellow crystals (0.77 g, 75%), m.p. 71°C. − ^{1}H NMR (200 MHz,

$CDCl_3$), δ = 8.95 (m, 1 H), 8.1 (m, 2 H), 7.6 (m, 2 H), 7.33 (d, *J* = 7.6 Hz, 1 H), 7.08 (d, *J* = 8.3 Hz, 2 H), 6.90 (d, *J* = 8.0 Hz, 2 H), 6.75 (s, 1 H), 4.41 (t, *J* = 6.7 Hz, 2 H), 3.38 (t, *J* = 5.6 Hz, 2 H), 3.14 (t, *J* = 5.6 Hz, 2 H), 2.67 (br. t, 2 H), 2.44 (t, 2 H), 2.28 (s, 3 H), 1.84 (m, 2 H), 1.3 (m, 22 H), 0.88 (t, *J* = 6.1 Hz, 3 H). – $C_{38}H_{51}NO_2$ (553.8): calcd. C 82.41, H 9.28, N 2.53; found C 82.52, H 9.11, N 2.46.

Tetradecyl 4-(1-p-Tolylpiperidin-4-ylmethyl)naphthalene-1-carboxylate (**2a**): The compound was synthesized as described for **1a**, starting with **2** (0.31 g, 0.57 mmol). Recrystallization from pentane yielded **2a** as white crystals (70 mg, 23%), m.p. 83°C. – ^{1}H NMR (200 MHz, $CDCl_3$), δ = 8.97 (m, 1 H), 8.1 (m, 2 H), 7.6 (m, 2 H), 7.33 (d, *J* = 7.5 Hz, 1 H), 7.06 (d, *J* = 8.4 Hz, 2 H), 6.87 (br. d, *J* = 7.6 Hz, 2 H), 4.40 (t, *J* = 6.1 Hz, 2 H), 3.57 (d, *J* = 12.7 Hz, 2 H), 3.07 (d, *J* = 6.6 Hz, 2 H), 2.58 (t, *J* = 11.5 Hz, 2 H), 2.26 (s, 3 H), 1.8 (m, 2 H), 1.4 (m, 22 H), 0.88 (t, *J* = 6.4 Hz, 3 H). – $C_{38}H_{53}NO_2$ (555.9): calcd. C 82.11, H 9.61, N 2.52; found: C 82.27, H 9.57, N 2.38.

4-[1-(4-Tetradecylphenyl)piperidin-4-ylidenemethyl]naphthalene-1-carbonitrile (**3**): Diethyl [(4-cyano-1-naphthyl)methyl]phosphonate (0.61 g, 2.0 mmol) was dissolved in THF (20 ml) under nitrogen. NaH (180 mg, 4.1 mmol) (55–60% suspension in paraffin oil) was added in portions. After 30 min, 1-(4-tetradecylphenyl)piperidin-4-one (0.74 g, 2.0 mmol) was added and the reaction mixture was stirred overnight. The brown suspension was poured into water (20 ml) and extracted with $CHCl_3$ (3 × 30 ml). After drying with magnesium sulfate, the solvent was evaporated, yielding a yellow-brown solid. The solid was dissolved in diethyl ether and gaseous HCl was led through the solution. After washing the white solid with diethyl ether and acetone, a potassium hydroxide solution was added and the suspension was extracted with CH_2Cl_2. After drying with magnesium sulfate, the solvent was evaporated, yielding a yellow solid. Recrystallization from ethanol yielded yellow needles (0.36 g, 35%), m.p. 66°C. – ^{1}H NMR (400 MHz, $CDCl_3$), δ = 8.27 (d, *J* = 8.1 Hz, 1 H), 8.12 (d, *J* = 8.3 Hz, 1 H), 7.89 (d, *J* = 7.4 Hz, 1 H), 7.71 (′t′, *J* = 7.6 Hz, 1 H), 7.63 (′t′, *J* = 7.6 Hz, 1 H), 7.35 (d, *J* = 7.2 Hz, 1 H), 7.08 (d, *J* = 8.5 Hz, 2 H), 6.89 (d, *J* = 8.4 Hz, 2 H), 6.73 (s, 1 H), 3.39 (t, *J* = 5.6 Hz, 2 H), 3.15 (t, *J* = 5.6 Hz, 2 H), 2.67 (t, *J* = 5.3 Hz, 2 H), 2.53 (t, *J* = 7.7 Hz, 2 H), 2.42 (t, *J* = 5.4 Hz, 2 H), 1.57 (m, 2 H), 1.3–1.2 (m, 22 H), 0.88 (t, *J* = 7 Hz, 3 H). – $C_{37}H_{48}N_2$ (520.8) : calcd. C 85.33, H 9.29, N 5.38; found C 85.45, H 9.23, N 5.28.

4-[1-(4-Tetradecylphenyl)piperidin-4-ylmethyl]naphthalene-1-carbonitrile (**3a**): A mixture of **3** (318 mg, 0.61 mmol), ethyl acetate (30 ml), PdH (39 mg) (10% on carbon), ethanol (15 ml) and two drops of 30% HCl was hydrogenated at 50 psi in a Parr apparatus for about 72 h. The catalyst was filtered off and the solvent was evaporated. A saturated sodium bicarbonate solution (10 ml) was added and the suspension was extracted with diethyl ether. The ether extracts were dried with magnesium sulfate; after filtration, the solvent was evaporated. The obtained white solid was purified by column chromatography on silica gel with CH_2Cl_2 and recrystallization from ethanol, yielding white needles (41 mg, 4%), m.p. 66°C. – ^{1}H NMR (400 MHz, $CDCl_3$): δ = 8.29 (“d”, *J* = 7.9 Hz, 1 H), 8.13 (“d”, *J* = 7.7 Hz, 1 H), 7.85 (“d”, *J* = 7.3 Hz, 1 H), 7.75–7.60 (m, 2 H), 7.36 (d, *J* = 6.7 Hz, 1 H), 7.05 (d, *J* = 8.6 Hz, 2 H), 6.86 (d, *J* = 8.3 Hz, 2 H), 3.60 (br. d, *J* = 12.4 Hz, 2 H), 3.10 (d, *J* = 7.0 Hz, 2 H), 2.59 (t, *J* = 11 Hz, 3 H), 2.51 (t, *J* = 7.7 Hz, 2 H), 1.84 (m, 1 H), 1.75 (br. d, *J* = 12.8 Hz, 2 H), 1.56 (m, 3 H), 1.4–1.2 (m, 22 H), 0.88 (t, *J* = 7 Hz, 3 H). – $C_{37}H_{50}N_2$ (522.8): calcd. C 85.00, H 9.64, N 5.36; found C 85.28, H 9.66, N 5.29.

[1] [1a] B. Wegewijs, *Long-range charge separation in solvent-free donor-bridge-acceptor systems. Donor-bridge-acceptor molecules in splendid isolation*, Ph. D. Thesis, University of Amsterdam, **1994**. – [1b] B. Wegewijs, R. M. Hermant, J. W. Verhoeven, A. G. M. Kunst, R. P. H Rettschnick, *Chem. Phys. Lett.* **1987**, *140*, 587. – [1c] B. Wegewijs, R. M. Hermant, J. W. Verhoeven, M. P. de Haas, J. M. Warman, *Chem. Phys. Lett.* **1990**, *168*, 185. – [1d] B. Wegewijs, A. K. F. Ng, R. P. H. Rettschnick, J. W. Verhoeven, *Chem. Phys. Lett.* **1992**, *200*, 357. – [1e] J. Jortner, M. Bixon, B. Wegewijs, J. W. Verhoeven, R. P. H. Rettschnick, *Chem. Phys. Lett.* **1993**, *205*, 451. – [1f] B. Wegewijs, T. Scherer, R. P. H. Rettschnick, J. W. Verhoeven, *Chem. Phys.* **1993**, *176*, 349. – [1g] B. Wegewijs, A. K. F. Ng, J. W. Verhoeven, *Recl. Trav. Chim. Pays-Bas* **1995**, *114*, 6. – [1h] B. Wegewijs, J. W. Verhoeven, S. E. Braslavsky, *J. Phys. Chem.* **1996**, *100*, 8890.

[2] [2a] T. Scherer, *Conformational dynamics of fluorescent exciplexes. On the structure of the emissive state in bridged donor-acceptor systems*, Ph. D. Thesis, University of Amsterdam, **1994**. – [2b] T. Scherer, R. J. Willemse, J. W. Verhoeven, *Recl. Trav. Chim. Pays-Bas* **1991**, *110*, 95. – [2c] J. W. Verhoeven, T. Scherer, R. J. Willemse, *Pure Appl. Chem.* **1993**, *65*, 1717. – [2d] W. Schuddeboom, T. Scherer, J. M. Warman, *J. Phys. Chem.* **1993**, *97*, 13092. – [2e] I. H. M. van Stokkum, T. Scherer, A. M. Brouwer, J. W. Verhoeven, *J. Phys. Chem.* **1994**, *98*, 852. – [2f] T. Scherer, I. H. M. van Stokkum, A. M. Brouwer, J. W. Verhoeven, *J. Phys. Chem.* **1994**, *98*, 10539.

[3] W. Jäger, S. Schneider, J. W. Verhoeven, *Chem. Phys. Lett.* **1997**, *270*, 50.

[4] T. Scherer, W. Hielkema, B. Krijnen, R. M. Hermant, C. Eijckelhoff, F. Kerkhof, A. F. K. Ng, R. Verleg, E. B. Van der Tol, A. M. Brouwer, J. W. Verhoeven, *Recl. Trav. Chim. Pays-Bas* **1993**, *112*, 535.

[5] J. W. Verhoeven, B. Wegewijs, R. M. Hermant, R. J. Willemse, A. M. Brouwer, *J. Photochem. Photobiol. A: Chem.* **1996**, *95*, 3–6.

[6] [6a] G. F. Mes, B. de Jong, H. J. van Ramesdonk, J. W. Verhoeven, J. M. Warman, M. P. de Haas, L. E. W. Horsman-van den Dool, *J. Am. Chem. Soc.* **1984**, *106*, 6524. – [6b] R. M. Hermant, N. A. C. Bakker, T. Scherer, B. Krijnen, J. W. Verhoeven, *J. Am. Chem. Soc.* **1990**, *112*, 1214. – [6c] R. M. Hermant, *Highly fluorescent donor-acceptor systems. Fundamentals and applications*, Ph. D. Thesis, University of Amsterdam, **1990**.

[7] [7a] E. Lippert, *Z. Naturforsch, A* **1955**, *10A*, 541. – [7b] E. Lippert, *Z. Elektrochem.* **1957**, *61*, 962. – [7c] N. Mataga, Y. Kaifa, M. Koizumi, *Bull. Chem. Soc. Jpn.* **1955**, *28*, 690. – [7d] N. Mataga, Y. Kaifa, M. Koizumi, *Bull. Chem. Soc. Jpn.* **1955**, *29*, 465.

[8] R. J. Willemse, *Photoinduced electron transfer in donor-acceptor systems with redox-active bridges*, Ph. D. Thesis, University of Amsterdam, **1997**.

[9] J. W. Verhoeven, T. Scherer, B. Wegewijs, R. M. Hermant, J. Jortner, M. Bixon, S. Depaemelaere, F. C. De Schryver, *Recl. Trav. Chim. Pays-Bas* **1995**, *114*, 443.

[10] I. R. Gould, R. H. Young, L. J. Mueller, A. C. Albrecht, S. Farid, *J. Am. Chem. Soc.* **1994**, *116*, 8188.

[11] K. A. Zachariasse, R. Busse, G. Duveneck, W. Kühnle, *J. Photochem.* **1985**, *28*, 237.

[12] H. Heitele, F. Pöllinger, S. Weeren, M. E. Michel-Beyerle, *Chem. Phys. Lett.* **1990**, *168*, 598

[13] [13a] M. P. de Haas, J. M. Warman, *Chem. Phys.* **1982**, *73*, 35. – [13b] J. M. Warman, M. P. de Haas, M. N. Paddon-Row, E. Cotsaris, N. S. Hush, H. Oevering, J. W. Verhoeven, *Nature* **1986**, *320*, 615. – [13c] J. M. Warman, S. A. Jonker, W. Schuddeboom, M. P. de Haas, M. N. Paddon-Row, J. W. Verhoeven, K. A. Zachariasse, *Pure Appl. Chem.* **1993**, *65*, 1723. – [13d] W. Schuddeboom, S. A. Jonker, J. M. Warman, U. Leinhos, W. Kühnle, K. A. Zachariasse, *J. Phys. Chem.* **1992**, *96*, 10809. – [13e] S. A. Jonker, J. M. Warman, *Chem. Phys. Lett.* **1991**, *185*, 36. – [13f] A. M. Brouwer, C. Eijckelhoff, R. J. Willemse, J. W. Verhoeven, W. Schuddeboom, J. M. Warman, *J. Am. Chem. Soc.* **1993**, *115*, 2988. – [13g] W. Schuddeboom, S. A. Jonker, J. M. Warman, M. P. de Haas, M. J. W. Vermeulen, W. F. Jager, B. de Lange, B. L. Feringa, R. W. Fessenden, *J. Am. Chem. Soc.* **1993**, *115*, 3286.

[14] M. P. de Haas, J. M. Warman, *Chem. Phys.* **1982**, *73*, 35.

[15] W. Schuddeboom, *Photophysical properties of opto-electric molecules studied by time-resolved microwave conductivity*, Ph. D. Thesis, Delft University, **1994**.

[16] A. L. McLellan, *Tables of experimental dipole moments*, vol. 3, Rahara Enterprises, El Cerrito, **1989**.
[17] S. L. Murov, I. Carmicheal, G. L. Hug, *Handbook of Photochemistry*, 2nd ed., Marcel Dekker Inc., New York, **1993**.
[18] D. D. Perrin, W. L. F. Armarego, D. R. Perrin, *Purification of Laboratory Chemicals*, 2nd ed., Pergamon Press Ltd., Oxford, **1980**.
[19] S. I. van Dijk, P. G. Wiering, C. P. Groen, A. M. Brouwer, J. W. Verhoeven, W. Schuddeboom, J. M. Warman, *J. Chem. Soc., Faraday Trans.* **1995**, *91*, 2107.
[20] D. W. Marquardt, *J. Soc. Ind. Appl. Math.* **1963**, *11*, 431.
[98206]